Surface Science 604 (2010) 623–626

Contents lists available at ScienceDirect

Surface Science

journal homepage: www.elsevier.com/locate/susc

Energy distributions in quasi-elastic peak electron spectroscopy

K. Tőkési *, D. Varga

Institute of Nuclear Research of the Hungarian Academy of Sciences (ATOMKI), H-4001 Debrecen, P.O. Box 51, Hungary

ARTICLE INFO

Article history:
Received 18 September 2009
Accepted for publication 11 January 2010
Available online 15 January 2010

Keywords:
Monte Carlo simulation
Multiple scattering
Elastic scattering

ABSTRACT

We present a theoretical description of the spectra of electrons elastically scattered from thin double layered Au–C samples. The analysis is based on very large scale Monte Carlo simulations of the recoil and Doppler effects in reflection and transmission geometries of the scattering at a fixed angle of 44.3° and a primary energy of 40 keV. The effect of the multiple scattering on intensity ratios, peak shifts and broadenings, for four cases of measurement geometry and layer thickness, are shown. Our Monte Carlo simulations are in good agreement with the experimental observations.

1. Introduction

In recent times the recoil energies of scattered electrons for atoms with large mass difference can be well resolved by using an energetic electron beam from a few keV range [1–3] to a few tens of keV [4–7]. This technique is called Electron Rutherford Backscattering Spectroscopy (ERBS), which relies on the quasi-elastic electron-atom scattering. In this case, we take advantage of the fact that the energy of the elastically scattered electrons is shifted from the primary values due to the momentum transfer between the primary electron and the target atoms (recoil effect). Thereby, the peak due to electrons scattered elastically splits into component peaks, which can be associated with the electrons scattered mainly from different target atoms of the sample, respectively. Furthermore, the thermal motion of the scattering atoms causes broadening in the primary electron energy distribution, usually referred to as Doppler broadening.

The signal of the elastically scattered electrons holds important information from the complex many-body interactions between the electrons and the target material. From the accurate determination of the full width at half maximum (FWHM) of the peaks, the average kinetic energy of the atoms in the solid can be determined. Moreover, from the accurate peak shape analysis we can determine the Compton profile [8] or we can prognosticate different fine interaction processes like, for example final state interactions. Applying electrons with higher energies ($E > 10$ keV), besides the fundamental research interest, can highlight important technical applications and may give data for analytics. For example, from the measurement of the relative peak intensities we can estimate the thickness of the layer where the signal originates. So far, many experiments have been done using both non-relativistic and relativistic primary electron energies. However, the detailed and critical theoretical analysis, taking into account the effect of the different types of scattering on the measurable quantity, and thereby the test of the validity of the single scattering approach used mostly in the interpretation of the experimental data, is still missing. In this work an accurate Monte Carlo simulation is presented for a double layer sample, in order to simulate the spectrum of elastically scattered electrons having 40 keV primary energy.

2. Theory

Our model is based on the following assumptions: (a) The sample consists of two homogeneous and amorphous layers with ideally flat surfaces and interface (see Fig. 1). (b) The inelastic mean free path (IMFP) within the given layer is constant, and it does not change even in the vicinity of the interface. (c) The surface losses in vacuum were not taken into account (which is reasonable in the case of 40 keV primary energy). (d) For the description of the elastic scattering cross sections we use the calculations for free atoms, solving the Dirac–Hartree–Fock–Slater wave functions [9]. (e) We suppose that the energy loss of elastically scattered electrons can be calculated within the impulse approximation. In this case the lost energy of the electron following one elastic collision on the static target atom can be calculated as:

$$E_{r0} = \frac{2mE_0}{M}\left(1+\frac{E_0}{2mc^2}\right)(1-\cos\theta_0), \tag{1}$$

where E_0 and θ_0 is the initial energy and the scattering angle of the electron, m and M is the rest mass of the electron and the target atom, c is the velocity of the light in vacuum. The factor,

* Corresponding author.
E-mail address: tokesi@atomki.hu (K. Tőkési).

0039-6028/$ - see front matter © 2010 Elsevier B.V. All rights reserved.
doi:10.1016/j.susc.2010.01.005

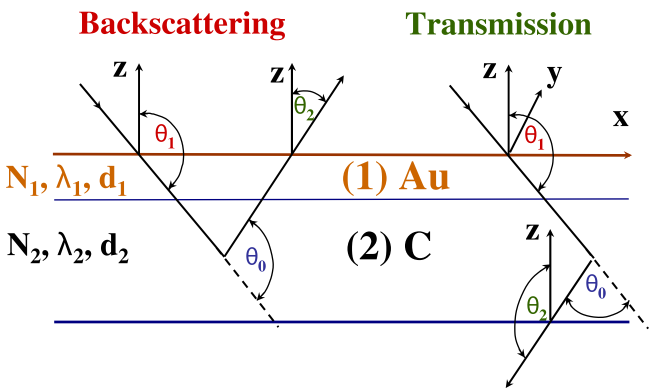

Fig. 1. Schematic view of the double layer Au–C sample and the geometry of the scattering used in our calculations. $\theta_0 = 44.3^\circ$ is the scattering angle. N_1 and N_2 are the atomic densities, λ_1 and λ_2 are the mean free paths and d_1 and d_2 are the thicknesses, layer by layer.

$(1 + \frac{E_0}{2mc^2})$, is the relativistic correction. For $E_0 = 40$ keV this relativistic correction causes a 3.9% increase. If we suppose that the target atom is moving, the energy loss after one elastic collisions (E_r) can be written as:

$$E_r = E_{r0}\left[1 + f(\vartheta, \varphi, \theta_0)\sqrt{\frac{M\varepsilon}{mE_0}\left(1 - \frac{E_0}{2mc^2}\right)}\right], \tag{2}$$

where $f(\vartheta, \varphi, \theta_0) = \cos\vartheta - \sin\theta_0 \sin\vartheta \cos\varphi(1 - \cos\theta_0)^{-1}$, ε is the kinetic energy of the moving target atom, ϑ and φ characterize the direction of the motion of the target atom with respect to the velocity of the primary electron and to the scattering plane, respectively. Furthermore, we suppose that the velocity distribution of the moving target atoms in the sample is isotropic and the kinetic energy can be described by the Maxwell–Boltzmann type function:

$$P(\varepsilon)d\varepsilon = \frac{3\sqrt{3}}{\sqrt{2\pi}}\frac{\sqrt{\varepsilon}}{\bar{\varepsilon}^{3/2}}\exp\left(-\frac{3\varepsilon}{2\bar{\varepsilon}}\right)d\varepsilon, \tag{3}$$

where $\bar{\varepsilon}$ is the average kinetic energy of the atoms in the given layer. This value can be selected freely, but at room temperature, in many cases, $\bar{\varepsilon}$ can have a value only a little higher than $\frac{3}{2}kT$.

The random motion of the electron in the sample is followed in the XYZ coordinate system (see Fig. 1). In the usual way, random numbers describe the distances between two scattering points, the type of the scattering (elastic or inelastic), and the scattering angle for the case of elastic collisions (θ, ϕ). The inelastic mean free paths (IMFP) differ significantly in the two layers, therefore, we take special care of the electrons crossing the interface in the accurate determination of IMFP. Furthermore, for the case of elastic collisions, the energy loss is also calculated by Eq. 2 using randomly generated angles, ϑ and φ, and by the help of randomly generated kinetic energy, ε, from the corresponding Maxwell–Boltzmann energy distribution.

3. Results and discussion

The Monte Carlo code was applied for four different cases, for two Au–C double layer samples in reflection and transmission mode. The first sample consisted of $d_1 = 1$ Å gold layer on the top of $d_2 = 90$ Å thick carbon foil and the second one consisted of $d_1 = 2$ Å gold layer on the top of carbon foil with thickness of $d_2 = 1400$ Å . Our recent choice of the primary energy, incident and scattering angles was highly motivated by the experimental data published in [5,6]. The incident angle, θ_1, was 112.15° in the reflection and 157.85° in the transmission geometry. According to the nominal value of the scattering angle ($\theta_0 = 44.3^\circ$, which was the same in all cases), the corresponding values of the emission angle (θ_2) were 67.85° in the reflection and 157.85° in the transmission geometry, respectively. Naturally, for the case of the real solid angle of the electron collection ($\Delta\Omega = 0.03$ sr) the values of the scattering and emission angles can vary within the allowed angles in the range of $\Delta\Omega$. We note that the angular dispersion for the incident beam was neglected in our simulation.

The other input data of the Monte Carlo simulations were as follow: The atomic densities are $\rho(\mathrm{Au}) = 19.3\ \mathrm{g/cm^3}$ and $\rho(C) = 2.0\ \mathrm{g/cm^3}$. The corresponding inelastic mean free paths are $\lambda_i(\mathrm{Au}) = 252.4$ Å and $\lambda_i(\mathrm{C}) = 530.3$ Å. The elastic mean free paths are $\lambda_e(\mathrm{Au}) = 48.5$ Å and $\lambda_e(\mathrm{C}) = 616.8$ Å. The total mean free paths are $\lambda(\mathrm{Au}) = 40.7$ Å and $\lambda(\mathrm{C}) = 285.1$ Å.

We used $\bar{\varepsilon} = 108$ meV for the average kinetic energy of the C atoms. This value corresponds to the value obtained from the neutron scattering experiments [10], and also with our findings using electron spectroscopy measurements [1]. We use $\bar{\varepsilon} = 40$ meV for the case of the gold target, because the Debye temperature is rather low for gold (165 K), and therefore it can not be expected to be significantly different compared to the value of $\frac{3}{2}kT$.

We performed *theoretical experiments* and we followed 10^{11} primary electron trajectories for each collision system. Besides the total yield and spectra of the elastically scattered electrons, many partial yields and spectra were also stored for the investigation of the effect of various type of scattering and geometry. The main parameters of the single scattering from double layered samples, such as scattering probabilities, peak shifts, and peak widths, can be calculated analytically [11]; therefore, we used two partial distributions, namely the energy distributions of the single scattering on gold and carbon atoms for the test of our Monte Carlo results. We found that the corresponding data are in excellent agreement with each other within 0.1%. With the help of three further partial distributions, (two distributions of the multiple scattering on the gold atoms only, and on the carbon atoms only, and finally the energy distribution of the multiple scattered electrons when both target atoms contribute to the process) the effect of the multiple scatterings on the intensity ratios of the gold and carbon peaks, the peak shifts and the peak widths were investigated.

In the real experimental condition the angular spread of the primary electron beam and the $\Delta\Omega$ angular range for the detection allows significant fluctuation in the scattering angle, and in the corresponding angular differential cross sections. This can influence the measured peak shift, width, shape, and area. Therefore, we also performed the numerical integration of the analytical expressions for single scattering supposing infinitesimally small solid angle, $d\Omega$, over the finite solid angle, $\Delta\Omega$. In our present case, the finite solid angle, $\Delta\Omega = 0.03sr$ was divided into 4000 solid angle elements (both in azimuth and polar angles, $d\Omega_{ij}$) and for all $d\Omega_{ij}$ the corresponding scattering angle, peak shifts, and width were calculated. Then, by using of the elementary yields as a weighting factor, the correct data for finite solid angle, $\Delta\Omega$, can be obtained. These data can differ from that of the data calculated using the nominal value of the scattering angle of $\theta_0 = 44.3^\circ$. In our present case, for the four Au and C peaks it gives 1–4% less yield, on average 3.6% higher peak separation and 2.7% higher peak widths in comparison with the real (integrated) values. We also compared the analytical results integrated over the finite solid angle $\Delta\Omega$ with the results of our Monte Carlo calculations for single scatterings. We found that the data are in agreement within the statistical fluctuation and in most of the cases this agreement better than 0.1%. We consider this excellent agreement as an additional accurate test of our Monte Carlo calculation for the case of the single scatterings. Integrating over the finite solid angle modifies the peak shape, and the peak become asymmetric. This can be seen in Fig. 2.

The shape of the curve ($\bar{\varepsilon} = 0$ meV) in Fig. 2 is determined mainly by the change of the differential elastic scattering cross sec-